



Supplementary Information for

Conformation and dynamic interactions of the multipartite genome
in *Agrobacterium tumefaciens*

Zhongqing Ren, Qin Liao, Xheni Karaboja, Ian S. Barton, Eli G. Schantz, Adrian Mejia-Santana,
Clay Fuqua, Xindan Wang

Xindan Wang
Email: xindan@indiana.edu

This PDF file includes:

Supplementary Materials and Methods
Figures S1 to S10
Tables S1 to S4
SI References

Supplementary Materials and Methods

Hi-C

The detailed Hi-C procedure for *A. tumefaciens* was adapted from a previously described *B. subtilis* protocol (1). Briefly, exponentially-growing cells were crosslinked with 3% formaldehyde at room temperature for 30 min then quenched with 125 mM glycine. 1.3×10^8 cells were used for each Hi-C reaction. Cells were lysed using Ready-Lyse Lysozyme (Epicentre, R1802M) followed by 0.5% SDS treatment. Solubilized chromatin was digested with HindIII for 2 hours at 37°C. The digested ends were filled in with Klenow and Biotin-14-dATP, dGTP, dCTP, dTTP. The products were ligated in dilute reactions with T4 DNA ligase at 16°C for about 20 hrs. Crosslinks were reversed at 65°C overnight for about 20 hrs in the presence of EDTA, proteinase K and 0.5% SDS. The DNA was then extracted twice with phenol/chloroform/isoamylalcohol (25:24:1) (PCI), precipitated with ethanol, and resuspended in 20 µl of 0.1XTE buffer. Biotin from non-ligated ends was removed using T4 polymerase (4 hrs at 20°C) followed by extraction with PCI. The DNA was then sheared by sonication for 12 min with 20% amplitude using a Qsonica Q800R2 water bath sonicator. The sheared DNA was used for library preparation with the NEBNext Ultrall kit (E7645) following the manufacturer's instructions for end repair, adapter ligation, and size selection. Biotinylated DNA fragments were purified using 10 µl streptavidin beads. DNA-bound beads were used for PCR in a 50 µl reaction for 14 cycles. PCR products were purified using Ampure beads (Beckman, A63881) and sequenced at the Indiana University Center for Genomics and Bioinformatics using NextSeq 550. Paired-end sequencing reads were mapped to the combined genome files of *A. tumefaciens* C58 (NCBI Reference Sequence GCA_000092025.1) using the same pipeline described previously (1). The combined *A. tumefaciens* C58 genome was divided into 568x10-kb. Subsequent analysis and visualization were done using R scripts. To put *ori1* at the center of Ch1, the reference genome of Ch1 starts at 1400 kb.

ChIP-seq

Chromatin immunoprecipitation (ChIP) for *A. tumefaciens* was performed similar to a previously described *B. subtilis* protocol (1) with minor modifications. Cells were crosslinked using 3% formaldehyde for 30 min at room temperature and then quenched, washed, and lysed. Chromosomal DNA was sheared to an average size of 250 bp by sonication using a Qsonica Q800R2 water bath sonicator. The lysate was precleared using 50 µl beads (GE HealthCare Protein A Meg Sepharose, 28978111-AB), then incubated with 4 µl of anti-ParB1 (this study, see below), anti-RepB^{Ch2} (this study, see below) or anti-GFP (2) antibodies at 4°C with rotation overnight. Then, lysates were incubated with the Protein A Meg Sepharose beads (28978111-AB) for 1 hr at 4°C. After washes and elution, the immunoprecipitate was incubated at 65°C overnight to reverse the crosslinks. The DNA was further treated with RNaseA, Proteinase K, extracted with PCI, resuspended in 100 µl 0.1x TE buffer and subjected to library preparation using the NEBNext Ultrall kit (E7645). The samples were sequenced using the Illumina NextSeq550 platforms. The sequencing reads were aligned to the combined *A. tumefaciens* C58 genome (NCBI GCA_000092025.1)

using CLC Genomics Workbench (CLC Bio, QIAGEN). Sequencing reads from ChIP and input samples were normalized by the total number of reads for each sample. The ChIP enrichment (ChIP/Input) was plotted in R.

Identification of *parS* sites

For ParB1, we searched the consensus sequence TGTTNCACGTGAAACA (3) allowing 2-3 mismatches across the whole genome. We identified 7 sites in the ParB1 enrichment region (40 kb) and none outside of this region. For RepB^{Ch2}, we used Emboss Palindrome program (<http://emboss.bioinformatics.nl/cgi-bin/emboss/palindrome>) to search 16-bp palindromes allowing 2 mismatches. We found 4 sites at the RepB^{Ch2} ChIP peaks on Ch2 with GTTNNCNGCNGNNAAC pattern (4). For RepB^{pTi}, the same pattern GTTNNCNGCNGNNAAC (4) was used to search for the *parS* sites with the allowance of 2 mismatches. We identified two sites: one in the intergenic region between *repA^{pTi}* and *repB^{pTi}* and the other inside *repB^{pTi}* gene.

Whole Genome Sequencing (WGS)

About 5x10⁸ exponentially growing cells were collected for WGS. The genomic DNA was purified using Qiagen Dneasy Kit (69504), sonicated for 12 min with 20% amplitude using a Qsonica Q800R2 water bath sonicator, prepared using the NEBNext Ultrall kit (E7645) and sequenced using Illumina NextSeq550. The reads were mapped to the *A. tumefaciens* C58 genome (NCBI GCA_000092025.1) using CLC Genomics Workbench (CLC Bio, QIAGEN). The mapped reads were normalized to the total number of reads, divided by the averaged total number of reads at the terminus of Ch1 to calculate the relative copy numbers, then plotted and analyzed using R scripts.

Fluorescence Microscopy

Fluorescence microscopy was performed on a Nikon Ti2E microscope equipped with Plan Apo 100x/1.4NA phase contrast oil objective and an sCMOS camera. For snapshot imaging, cells were immobilized using 2% agarose pads containing growth media. Images were cropped and adjusted using MetaMorph software (Molecular Devices). Final figures were prepared in Adobe Illustrator. For time-lapse imaging, a glass-bottomed dish (Willco dish HBSt-5040; Willco Wells) was used as a coverslip. Exponentially growing cells were concentrated at 4,600 × g for 30 s. After removal of 90% of the supernatant, 2 μL of the culture was spotted onto the glass-bottomed dish. A 2% agarose pad containing growth media was then laid on top of the bacteria. These cells were imaged on a Okolab Uno stage top incubator with temperature controller (H301) and objective heater (OBJ-T). The upper face of the pad was fully exposed, allowing adequate oxygen for growth. Images were acquired every 10 min. When appropriate, 0.25 mM of IPTG was added to induce the expression of fluorescently-tagged ParB1 or RepB proteins.

Image analysis

Image analyses were performed using the MathWorks MATLAB-based program Oufiti (5). Cell outline were detected using the cellDetection module. Localizations of fluorescent foci were identified using the spotDetection module. Pre-Gaussian parameters were set as the following: wavelet scale = 0, low pass = 2, spot radius = 2, int. threshold = 0.4, min region size = 4, fit radius = 2. Post-Gaussian parameters were minHeight = 0, minWidth = 1.9, maxWidth = 10, Adjusted Squared Error = 0. The same parameters were used for all strains. For the plots in Fig. 3AB, the x-axis indicated the cell length; the y-axis indicated the position of foci, where 0 was the mid-cell and the “negative” was the cell pole that was closer to a fluorescent focus. After cellDetection and spotDetection, manual inspection was employed to remove the cell meshes with wrongly detected cell outline or spots. To prevent the plots from being too crowded, for samples that had over 1000 cells, only the first 1000 cells in the cellList were shown. The data were further analyzed and plotted in MATLAB (Figs. 3CD, S8, S9C).

Generation of ParB1 and RepB^{Ch2} antibodies

His6-ParB1 and His6-RepB^{Ch2} were expressed in *E. coli* BL21 DE3 pLysS. Cells were grown in LB at 37°C to an OD₆₀₀ of 0.4 and induced with 0.5 mM IPTG for 2 hrs. All subsequent manipulations were carried out at 4°C. 250 mL of cells were harvested by centrifugation and resuspended in 20 mL lysis buffer (50 mM HEPES Na⁺ pH 8.0, 500 mM NaCl, 5 mM b-Mercaptoethanol, 10 mM imidazole). A crude extract was prepared by freeze-thawing the cells followed by the addition of 1 mM PMSF and 0.5 mg/ml Lysozyme, and then sonication using a microtip sonicator at 40% duty, 20s on, 60s off on ice for 5 rounds in total. The lysates were centrifuged at 100,000 g for 1 hour. The soluble fraction was then loaded onto a 3 mL Ni²⁺-NTA agarose (QIAGEN) column equilibrated with lysis buffer. Bound proteins were washed with wash buffer (20 mM HEPES Na⁺ pH 8.0, 500 mM NaCl, 5 mM b-Mercaptoethanol, 50 mM Imidazole, 10% glycerol) followed by elution in elution buffer (20 mM HEPES Na⁺ pH 8.0, 500 mM NaCl, 5 mM b-Mercaptoethanol, 500 mM Imidazole, 10% glycerol). Peak fractions were pooled and dialyzed with three changes into dialysis buffer (20 mM HEPES K⁺ pH 7.6, 50 mM KCl, 1mM EDTA, 10% glycerol, 5 mM b-Mercaptoethanol). Protein concentrations were determined using the Bradford reagent from Thermo Scientific. The purified proteins were sent to Josman LLC to generate polyclonal antibodies from rabbit using a 56-day protocol. One animal was used for each protein.

Immunoblot analysis

Western blotting for *A. tumefaciens* was performed similar to previously described (1). Exponentially growing cells were collected and resuspended in sample buffer (Bio-Rad 1610737) containing 10% 2-Mercaptoethanol to achieve an OD₆₀₀ of 10 for equal loading. Samples were heated for 5 min at 95°C and vortexed vigorously for 30 seconds before loading to denature the proteins and shear the genomic DNA. Proteins were separated by precast 4-20% polyacrylamide gradient gels (Bio-Rad 4561096), electroblotted onto mini PVDF membranes using Bio-Rad Transblot Turbo system and reagents (Bio-Rad

1704156). The membranes were blocked in 5% nonfat milk in phosphate-buffered saline (PBS) with 0.5% Tween-20, then probed with anti-ParB1 (1:10,000), anti-RepB^{Ch2} (1:10,000) or anti-PruR (6) (1:4,000) diluted into 3% BSA in 1x PBS-0.05% Tween-20. Primary antibodies were detected using Immun-Star horseradish peroxidase-conjugated goat anti-rabbit antibodies (Bio-Rad 1705046) and Western Lightning Plus ECL chemiluminescence reagents as described by the manufacturer (Perkin Elmer NEL1034001). The signal was captured using ProteinSimple Fluorchem R system. The intensity of the bands were quantified using FIJI.

Plasmid construction

pWX820 [pSRKKm *msfgfp-parB1* (Atu2828/ATU_RS13770) (*kan*)] was constructed by an isothermal assembly reaction containing three gel-purified fragments: 1) pSRKKm (7) digested by NdeI and HindIII; 2) *msfgfp* amplified using oWX2044 and oWX2046 from pSRKKm *msfgfp* (8); 3) *At parB1* (Atu2828/ATU_RS13770) amplified using oWX2047 and oWX2048 from C58 genomic DNA. The construct was sequenced using oWX1835, oWX2060 and oWX2061.

pWX821 [pSRKKm *msfgfp-repB^{Ch2}* (Atu3923/ATU_RS18280) (*kan*)] was constructed by an isothermal assembly reaction containing three gel-purified fragments: 1) pSRKKm (7) digested by NdeI and HindIII; 2) *msfgfp* amplified using oWX2044 and oWX2046 from pSRKKm *msfgfp* (8); 3) *At repB^{Ch2}* (Atu3923/ATU_RS18280) amplified using oWX2049 and oWX2050 from C58 genomic DNA. The construct was sequenced using oWX1835, oWX2060 and oWX2061.

pWX832 [pNPTS138 Δ *smc* (Atu0801/ATU_RS03945) (*kan*)] was constructed by an isothermal assembly reaction containing three gel-purified fragments: 1) pNPTS138 (9) digested by EcoRV; 2) *At smc* (Atu0801/ATU_RS03945) upstream region amplified using oWX2081 and oWX2082 from C58 genomic DNA; 3) *At smc* downstream region amplified using oWX2083 and oWX2084 from C58 genomic DNA. The construct was sequenced using oWX1854 and oWX1855.

pWX844 [pSRKKm *mYpet-repB^{Ch2}* (Atu3923/ATU_RS18280) (*kan*)] was constructed by an isothermal assembly reaction containing two gel-purified fragments: 1) pWX821 digested by NdeI and BamHI; 2) *mYpet* amplified using oWX2169 and oWX2171 from pWX361 (10). The construct was sequenced using oWX1835, oWX2060 and oWX2173.

pWX854 [pNPTS138 Δ *repB^{Ch2}* (Atu3923/ATU_RS18280)::*amp* (*kan*)] was constructed by an isothermal assembly reaction containing four gel-purified fragments: 1) EcoRV-digested pNPTS138 (9); 2) *At repB^{Ch2}* (Atu2923) upstream region amplified using oWX2076 and oWX2206 from C58 genomic DNA; 3) *At repB^{Ch2}* downstream region amplified using oWX2207 and oWX2077 from C58 genomic DNA; 4) *amp*

amplified using oWX2210 and oWX2211 from plasmid pHP45omega (11). The construct was sequenced using oWX1854 and oWX1855.

pWX879 [pMiniTn7 *Ptral* MCS *traR* (*gen*)] was constructed by an isothermal assembly reaction containing two gel-purified fragments: 1) pUC18-mini-Tn7T-GM-Plac-HA (8) digested by Sall and NheI; 2) *Plac* MCS *traR* amplified using oWX2265 and oWX2266 from pTD114 (12). The construct was sequenced using oWX2031 and oWX2265.

pWX885 [pMiniTn7 *Ptral-riboswitch-parB1*(Atu2828/ATU_RS13770) *traR* (*gen*)] was constructed by an isothermal assembly reaction containing three gel-purified fragments: 1) pWX879 digested by XmaI and BamHI; 2) *riboswitch* amplified using oWX2288 and oWX2289 from pJZ274 (13); 2) *At parB1* amplified using oWX2268 and oWX2290 from C58 genomic DNA. The construct was sequenced using oWX2265 and oWX2273.

pWX902 [pNPTS138 *tetRA:: gen Ptral-riboswitch-parB1*(Atu2828/ATU_RS13770) *traR* (*kan*)] was constructed by an isothermal assembly reaction containing two gel-purified fragments 1) pMEH0125 (8) cut with NheI and NcoI; 2) *gen Ptral riboswitch parB1 traR* amplified using oWX2342 and oWX2343 from pWX885. The construct was sequenced using oWX2279, oWX2280, oWX2337, oWX2342, oWX2343, oWX2348 and oWX2349.

pWX905 [pSRKKm *mYpet-repB^{pAt}* (Atu5001/ATU_RS23955) (*kan*)] was constructed by an isothermal assembly reaction containing two gel-purified fragments: 1) pWX844 digested by XhoI and BamHI; 2) *At repB^{pAt}* (Atu5001/ATU_RS23955) amplified using oWX2405 and oWX2351 from C58 genomic DNA. The construct was sequenced using oWX1835 and oWX2173.

pWX906 [pSRKKm *mYpet-repB^{pTi}* (Atu6044/ATU_RS23220) (*kan*)] was constructed by an isothermal assembly reaction containing two gel-purified fragments: 1) pWX844 digested by XhoI and BamHI; 2) *At repB^{pTi}* (Atu6044/ATU_RS23220) amplified using oWX2406 and oWX2353 from C58 genomic DNA. The construct was sequenced using oWX1835 and oWX2173.

pWX914 [pNPTS138 Δ *parB1*(Atu2828/ATU_RS13770)::*amp* (*kan*)] was constructed by an isothermal assembly reaction containing four gel-purified fragments: 1) EcoRV-digested pNPT138 (9); 2) *At parB1* (Atu2828/ATU_RS13770) upstream region amplified using oWX2017 and oWX2380 from C58 genomic DNA; 3) *amp* amplified using oWX2381 and oWX2382 from plasmid pHP45omega (11); 3) *At parB1* downstream region amplified using oWX2383 and oWX2020 from C58 genomic DNA. The construct was sequenced using oWX1854 and oWX1855.

pWX917 [pACYC terminators Ppen *yGFP-parB^{MT1}-parS^{MT1}*] was constructed by an isothermal assembly reaction containing three gel-purified fragments: 1) pWX915 digested by HindIII and BamHI; 2) *yGFP-parB^{MT1}* amplified using oWX2391 and oWX2392 from pFHC2973 (14); 3) *parS^{MT1}* amplified using oWX2393 and oWX2394 from *Vibrio cholerae* SAD1924 gDNA(15). The construct was sequenced using oWX2377, oWX2395, oWX2396, and oWX2397. pWX915 is an empty cloning vector with a pACYC origin and transcription terminators, upstream of a Ppen promoter.

pWX924 [pACYC terminators Ppen *yGFP-parB^{MT1}-parS^{MT1} terminators*] was generated by a two-way ligation. The vector was from pWX197 digested with Sall and EagI. The insert was transcription terminators amplified from pWX361(10) using oWX2403 and oWX2404 then digested using Sall and EagI. The construct was sequenced using oWX2395.

pWX931 [pNPTS138 Ppen *yGFP-parB^{MT1}-parS^{MT1}* at Atu3054/ATU_RS14060] was constructed by an isothermal assembly reaction containing four gel-purified fragments: 1) EcoRV-digested pNPT138 (9); 2) Atu3054/ATU_RS14060 upstream amplified using oWX2420 and oWX2421 from C58 genomic DNA; 3) a part of Atu3054/ ATU_RS14060 amplified using oWX2422 and oWX2423 from C58 genomic DNA; 4) Ppen *yGFP-parB^{MT1}-parS^{MT1}* cassette amplified using oWX2407 and 2408 from pWX924. The construct was sequenced using oWX2379, oWX2424, oWX2425, and oWX2426.

pWX950 [pNPTS138 PT7strong *yGFP-parB^{MT1}-parS^{MT1}* at Atu3054/ATU_RS14060] was constructed by replacing the Ppen promoter in pWX931 with a PT7 strong promoter (16). This was done by using oWX2431 and oWX2432 to amplify the pWX931. The construct was sequenced using oWX2379, oWX2424, oWX2425, and oWX2426.

pWX963 [pNPTS138 PT7strong *yGFP-parB^{MT1}-parS^{MT1}* at Atu0048/ATU_RS00235] was constructed by an isothermal assembly reaction containing four gel-purified fragments: 1) EcoRV-digested pNPT138 (9); 2) Atu0048/ATU_RS00235 downstream amplified using oWX2502 and oWX2503 from C58 genomic DNA; 3) a part of Atu0048/ATU_RS00235 amplified using oWX2504 and oWX2505 from C58 genomic DNA; 4) *yGFP-parB^{MT1}-parS^{MT1}* cassette amplified using oWX2407 and 2408 from pWX950. The construct was sequenced using oWX2506, oWX2379, oWX2426 and oWX2507.

pWX967 [pNPTS138 PT7strong *yGFP-parB^{MT1}-parS^{MT1}* at Atu3973/ATU_RS18530] was constructed by an isothermal assembly reaction containing four gel-purified fragments: 1) EcoRV-digested pNPT138 (9); 2) Atu3973/ATU_RS18530 downstream amplified using oWX2508 and oWX2509 from C58 genomic DNA; 3) a part of Atu3973/ATU_RS18530 amplified using oWX2510 and oWX2511 from C58 genomic DNA; 4) *yGFP-parB^{MT1}-parS^{MT1}* cassette amplified using oWX2407 and 2408 from pWX963. The construct was sequenced using oWX2512, oWX2379, oWX2426 and oWX2513.

pWX970 [pSRKKm *Plac rfp-repB^{Ch2}* (Atu3923/ATU_RS18280) terminator *Plac egfp-parB1* (Atu2828/ATU_RS13770) terminators] was constructed by an isothermal assembly reaction containing three gel-purified fragments: 1) pACE001 (17) backbone amplified using oWX2520 and oWX2521 from pACE001; 2) *egfp At parB1* amplified using oWX2524 and oWX2525 from pJZ254 (17); 3) *rrmB terminators* (10)). The construct was sequenced using oWX2522 and oWX2524. Note this construct has *Plac rfp-repB^{Ch2}* and *Plac egfp-parB1* in converging direction separated by bi-directional terminators.

pWX974 [pSRKKm *Plac rfp-repB^{pAt}* (Atu5001/ATU_RS23955) terminator *Plac egfp-parB1* (Atu2828/ATU_RS13770) terminators] was constructed by an isothermal assembly reaction containing two gel-purified fragments: 1) pSRKKm *Plac rfp terminator Plac egfp-parB1* (Atu2828/ATU_RS13770) terminators backbone amplified using oWX2535 and oWX2536 from pWX970; 2) *repB^{pAt}* amplified using oWX2540 and oWX2541 from C58 genomic DNA. The construct was sequenced using oWX2539. Note this construct has *Plac rfp-repB^{pAt}* and *Plac egfp-parB1* in converging direction separated by bi-directional terminators.

pWX1004 [pNPTS138 *yGFP-parB^{MT1}-parS^{MT1}* at Atu6047/ATU_RS23235] was constructed by an isothermal assembly reaction containing four gel-purified fragments: 1) EcoRV-digested pNPT138 (9); 2) Atu6047/ATU_RS23235 downstream amplified using oWX2595 and oWX2596 from C58 genomic DNA; 3) a part of Atu6047/ATU_RS23235 amplified using oWX2593 and oWX2594 from C58 genomic DNA; 4) *yGFP-parB^{MT1}-parS^{MT1}* cassette amplified using oWX2407 and 2408 from pWX963. The construct was sequenced using oWX2379, oWX2407, oWX2408 and oWX2426.

pWX1005 [pNPTS138 *yGFP-parB^{MT1}-parS^{MT1}* Atu5337/ATU_RS25505] was constructed by an isothermal assembly reaction containing four gel-purified fragments: 1) EcoRV-digested pNPT138 (9); 2) Atu5337/ATU_RS25505 downstream amplified using oWX2599 and oWX2600 from C58 genomic DNA; 3) a part of Atu5337/ATU_RS25505 amplified using oWX2597 and oWX2598 from C58 genomic DNA; 4) *yGFP-parB^{MT1}-parS^{MT1}* cassette amplified using oWX2407 and 2408 from pWX963. The construct was sequenced using oWX486, oWX2378, oWX2379 and oWX2407.

pWX1025 [pSRKKm *mYpet-repB^{pTi}(parS*)* (Atu6044/ATU_RS23220) (*kan*)] was constructed by an isothermal assembly reaction containing three gel-purified fragments: 1) pWX906 digested by XhoI and NdeI; 2) *At repB^{pTi}(parS*)* (Atu6044/ATU_RS23220) amplified using oWX2712 and oWX2169 from pWX906 and 3) *mYpet* amplified using oWX2713 and oWX2169 from pWX906. The construct was sequenced using oWX oWX2173.

Strain construction

In general, in-frame deletions of C58 *A. tumefaciens* strains were constructed using a previously described allelic replacement method (18). Briefly, regions flanking the gene to be deleted were PCR amplified using Phusion (NEB M0530) or Q5 polymerase (NEB M0491) and cloned into pNPTS138 (9), a ColE1 suicide plasmid that confers kanamycin resistance and sucrose sensitivity, by isothermal assembly reactions. See Plasmid Construction section for details. The pNPTS138 deletion plasmids were then introduced into *A. tumefaciens* C58 via mating with *E. coli* S17-1/λpir (19) carrying the appropriate construct. Screening for plasmid integration and target gene deletion was performed as previously described (18, 20). The deletion mutants were confirmed by colony PCR. Specific information about each strain can be found below.

Δsmc (AtWX108) was generated using pWX832, and confirmed using oWX2085 and oWX2086.

ΔrepB^{Ch2}::amp (AtWX089) was generated using pWX854. We note that for this strain, we used *amp* resistance gene to replace *repB^{Ch2}*. It was constructed similarly to the deletion constructs, except that at the step of secondary selection of plasmid loop-out, carbenicillin was added to plates and liquid media to force looping out the target gene instead of reversing to the wild-type. More specifically, the primary integrants that are resistant to both carbenicillin and kanamycin and sensitive to sucrose, were growing overnight to reach exponential phase, and then plated on sucrose plates supplied with carbenicillin. The colonies that are resistant to both sucrose and carbenicillin but sensitive to kanamycin were the candidates of the mutant. Colony PCR using oWX2021 and oWX2024 were used to confirm the allelic replacement.

tetRA::gen P_{tral-riboswitch}-parB1(Atu2828/ATU_RS13770) traR (AtWX192/AtWX193) isolates were constructed in three steps. First, pJW101 was used to delete *tral*, generating AtWX113, which was confirmed using oWX2276 and oWX2277. Then pWX902 was used to replace *tetRA* locus with the *gen P_{tral-riboswitch}-parB1(Atu2828/ATU_RS13770) traR* cassette, generating AtWX167, which was confirmed using oWX2279 and oWX2280. Finally, the endogenous *parB1* was deleted using pWX914, generating AtWX192 and AtWX193, which were confirmed using oWX2017 and oWX2020.

yGFP-parB^{MT1}-parS^{MT1} inserted between Atu0047/ATU_RS00230 and Atu0048/ATU_RS00235 50 kb from ori1 (AtWX278) was generated using pWX963, and confirmed using oWX2502 and oWX2505.

yGFP-parB^{MT1}-parS^{MT1} inserted between Atu3973/ATU_RS18530 and Atu3974/ATU_RS18535 57 kb from ori2 (AtWX295) was generated using pWX967, and confirmed using oWX2508 and oWX2511.

yGFP-parB^{MT1}-parS^{MT1} inserted between Atu5336/ATU_RS25500 and Atu5337/ATU_RS25505 11 kb from oAt (AtWX359) was generated using pWX1005, and confirmed using oWX2597 and oWX2600.

***yGFP-parB^{MT1}-parS^{MT1}* inserted between *Atu6047/ATU_RS23235* and *Atu6048/ATU_RS23240* 4 kb from *oTi* (**AtWX351**) was generated using pWX1004, and confirmed using oWX2593 and oWX2596.**

For strains containing plasmids for visualization, pWX820, pWX821, pWX905, pWX906, pWX970, pWX974 and pWX1025 were directly electroporated into WT C58 (*AtWX063*), as previously described (18) to generate *AtWX226*, *AtWX228*, *AtWX179*, *AtWX181*, *AtWX263*, *AtWX319* and *AtWX372*.

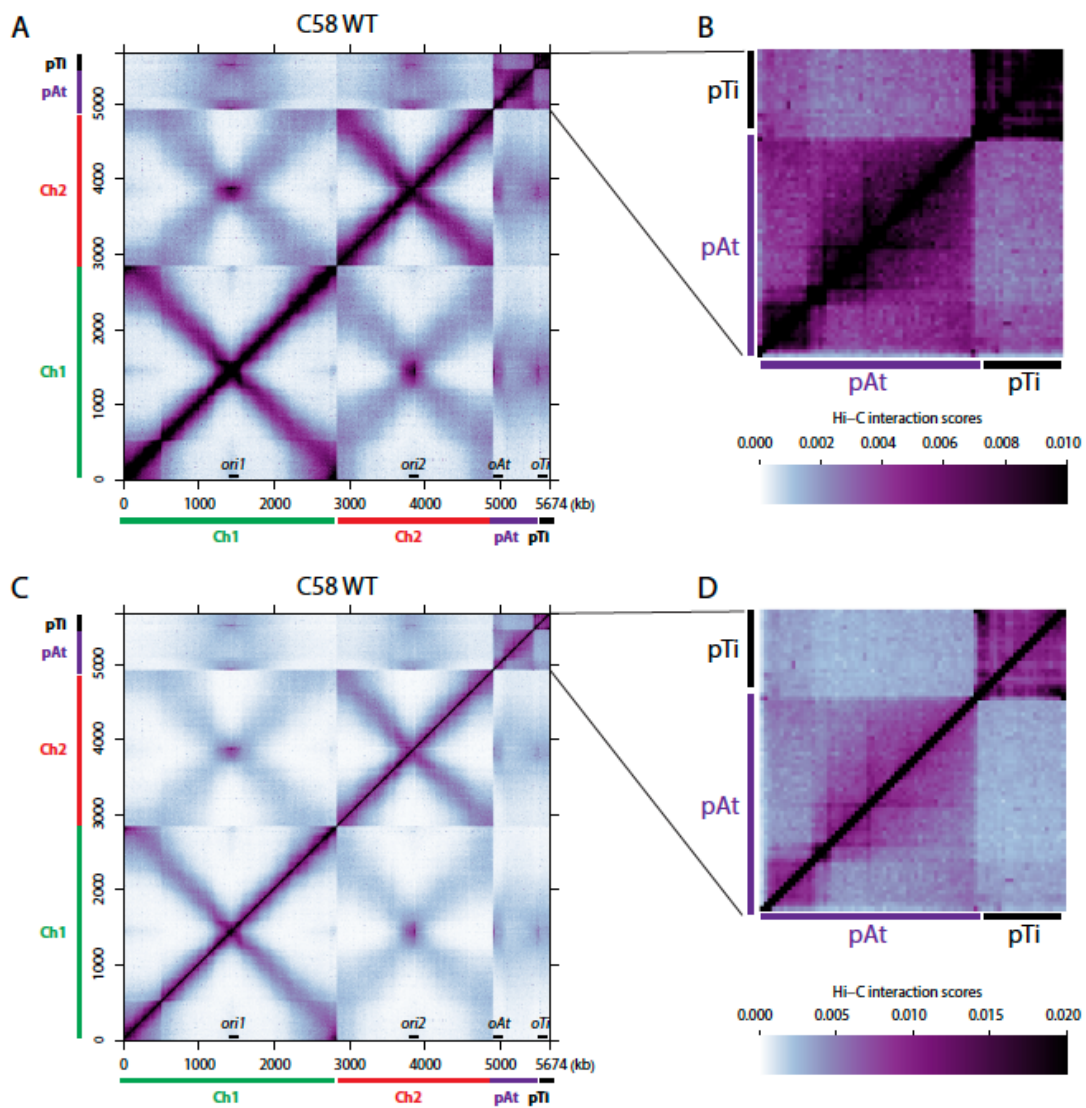


Fig. S1. pAt and pTi do not have inter-arm interactions. (A) Normalized Hi-C contact maps for C58 WT growing in ATGN. (B) Top, a high-resolution view of the plasmids. Bottom, the color scale bar. (C-D) the same data plotted using a different color scale. Inter-arm interactions are absent in pAt and pTi.

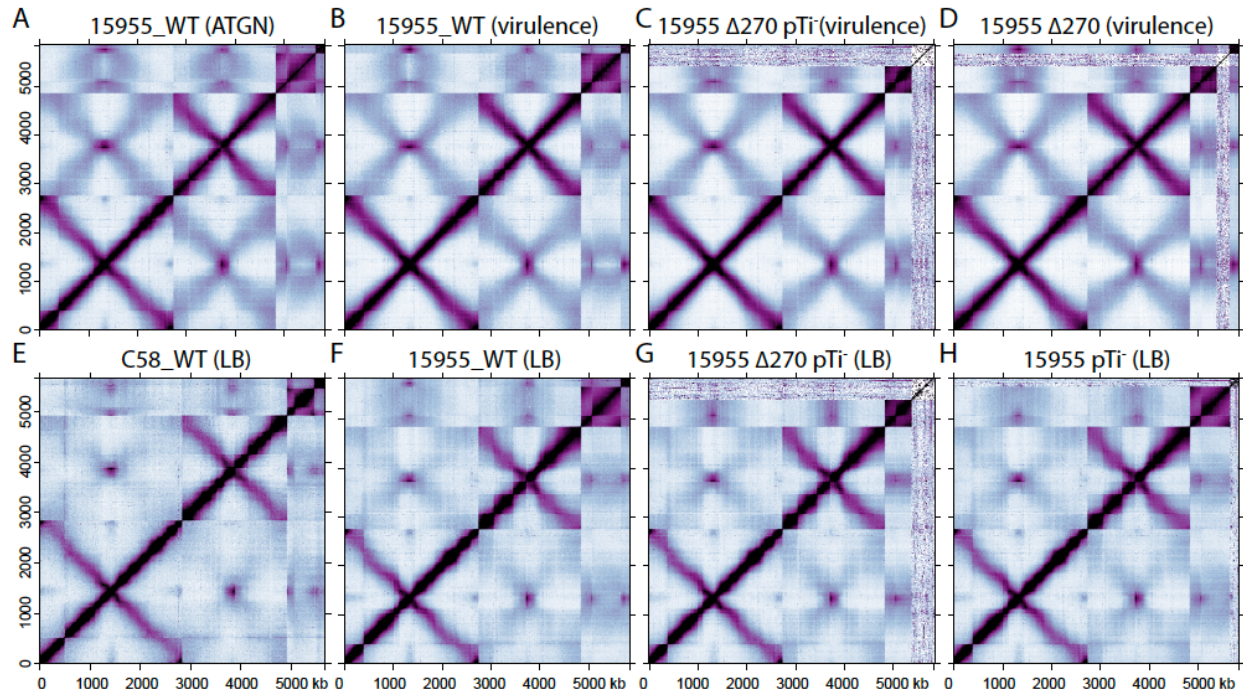


Fig. S2. Comparison of different *A. tumefaciens* derivatives growing in different conditions. (A-H) Normalized Hi-C contact maps for (A) 15955 WT (ATGN), (B) 15955 WT (virulence induction broth), (C) 15955 Δ 270 pTi⁻ (virulence induction broth), (D) 15955 Δ 270 (virulence induction broth), (E) C58 WT (LB), (F) 15955 WT (LB), (G) 15955 Δ 270 pTi⁻ (LB), (H) 15955 pTi⁻ (LB). C58 or 15955 derivatives were grown in rich medium (LB), minimal medium (ATGN), or virulence induction broth. 15955 Δ 270 pTi⁻ (IB124) has a 270-kb region on pAt deleted and whole pTi cured. 15955 Δ 270 (IBE13A) has the same 270-kb region deletion as IB124. 15955 pTi⁻ (IBJUN138) has pTi cured.

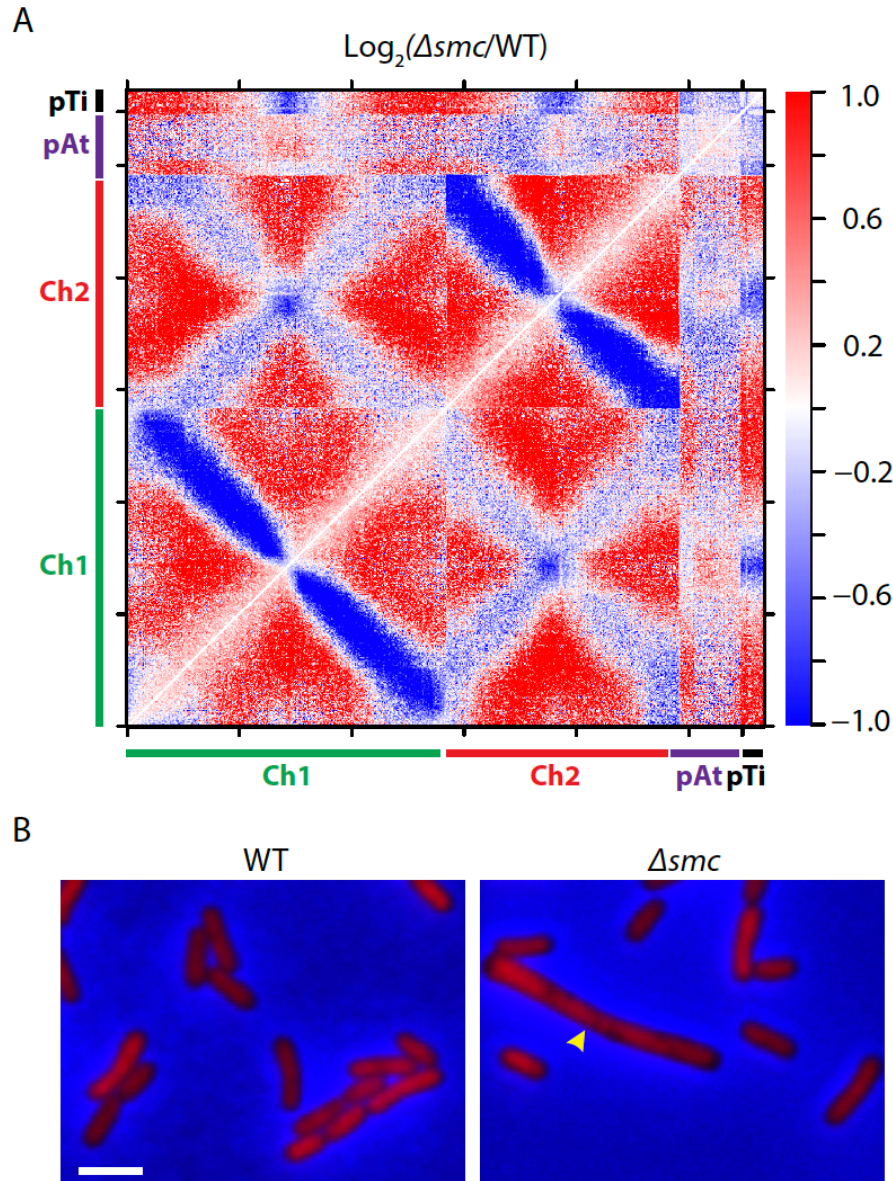


Fig. S3. Changes of chromosome conformation in a Δsmc mutant. (A) Log_2 ratio comparison of normalized contact maps binned at 10 kb: Δsmc (AtWX108, Fig. 1E) vs WT (AtWX063, Fig. 1B). The x-axis and y-axis show genome positions, with green, red, purple and black bars indicating the positions of Ch1, Ch2, pAt and pTi, respectively. The scale bar on the right depicts $\text{log}_2(\Delta smc/WT)$. Dark blue color indicates reduced interactions in Δsmc , red color indicates enhanced interactions in Δsmc , and white color indicates no change. In Δsmc , the inter-arm interactions within Ch1 and Ch2 are greatly reduced, but the inter-chromosomal interactions are largely unaltered. (B) Δsmc mutant has mild chromosome segregation defect. Wildtype (AtWX063) and Δsmc (AtWX108) were grown in ATGN liquid medium in exponential phase at 30°C. DAPI (2 $\mu\text{g}/\text{ml}$) stained nucleoid are shown in red. Scale bar indicates 2 μm . In the Δsmc mutant, we observed 7 out of 553 cells (1.3%) with extra long length (see below) and unsegregated nucleoid (yellow caret), whereas in the wild-type, we observed 0 out of 639 cells (0%) with the same phenotype. We define “extra long” cells as those greater than 4.25 μm , which is 2.17 μm + 4x0.52 μm , where 2.17 μm and 0.52 μm are respectively the mean and standard deviation of WT cell length (n=639).

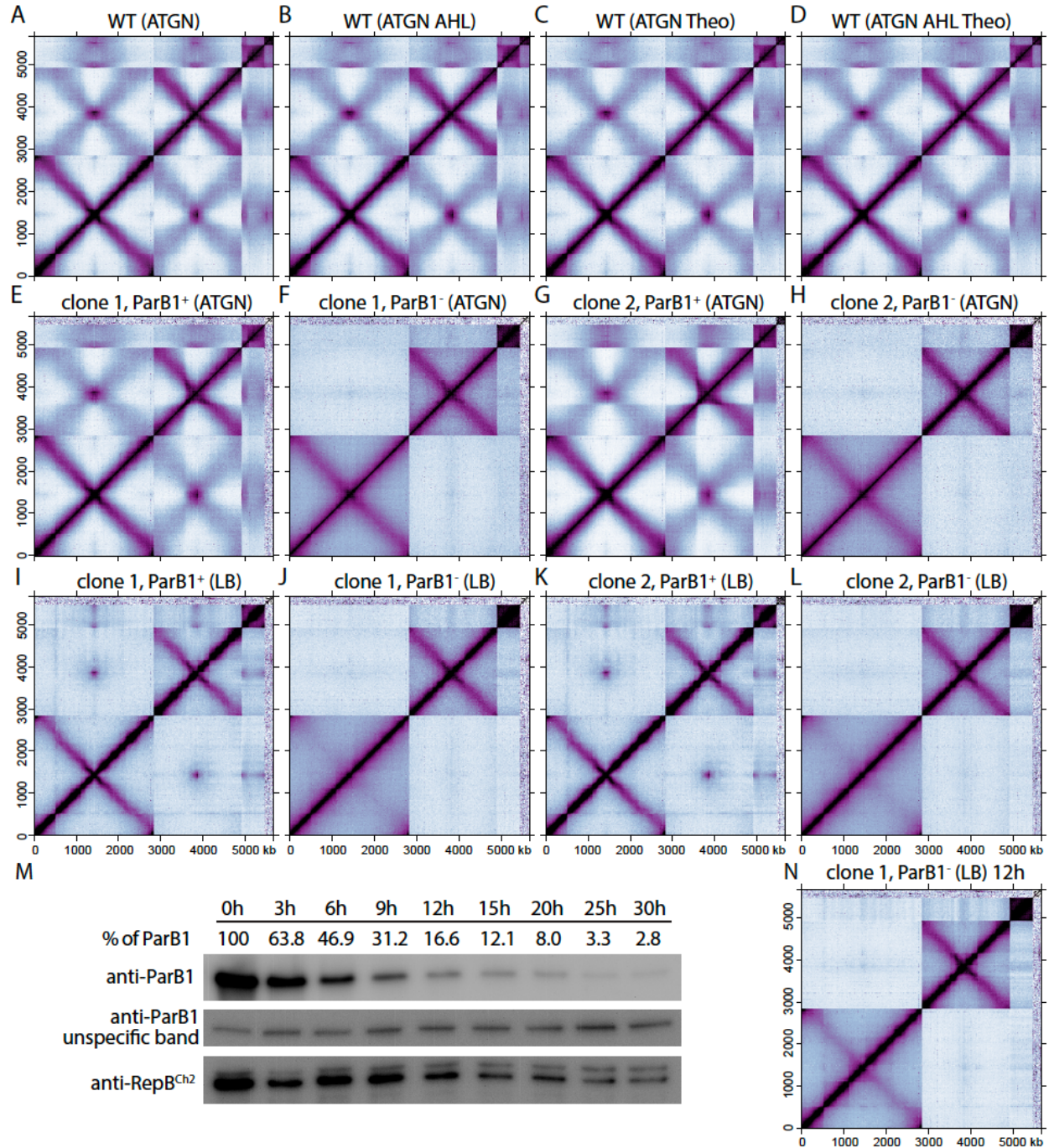


Fig. S4. Comparison of ParB1 depletion in ATGN and LB. (A-D) Normalized Hi-C contact maps for WT C58 cells (*AtWX063*) grown in (A) ATGN only, or also containing (B) AHL, or (C) theophylline, or (D) with AHL and theophylline. AHL and theophylline were added at 1 μ M and 2 mM, respectively. Addition of AHL and theophylline did not alter the chromosome interaction pattern. (E-H) Normalized Hi-C contact maps for ParB1 depletion strains grown in ATGN. Two independent genetic isolates, clone 1 (*AtWX192*) and clone 2 (*AtWX193*) are shown. ParB1⁺ condition was with AHL and theophylline. ParB1⁻ condition was without those inducers for 30 hours. (I-L) Same as (E-H) but grown in LB. When ParB1 was depleted for 30 hours, inter-arm interactions on Ch1 were reduced in ATGN (E-H), but were completely absent in LB (I-L). We note that inter-replicon interactions (*ori-ori* clustering and Ch1-Ch2 alignment) are less

pronounced in LB (Fig. S2E) compared with those in ATGN (A); pTi was lost from both clones of the ParB1 depletion strain. (M) Immunoblot analysis of ParB1 depletion time course. The levels of ParB1, an unspecific band using ParB1 antibodies, and the levels of RepB^{Ch2} are shown. ParB1 depletion strain (AtWX192) was grown in LB containing 1 μ M AHL and 2 mM theophylline on solid media or in liquid media. To deplete ParB1, cells were washed in LB medium for 4 times, then diluted to fresh LB without inducers. Cultures were diluted before their OD₆₀₀ reached 0.8 to prevent cells from entering stationary phase. Samples were taken at the indicated time points. The intensity of the bands were quantified using FIJI. (N) ParB1 depletion (AtWX192) in LB for 12 hours (~86% depleted according to (M)) gave intermediate result, i.e. inter-arm interactions on Ch1 were reduced but not completely absent.

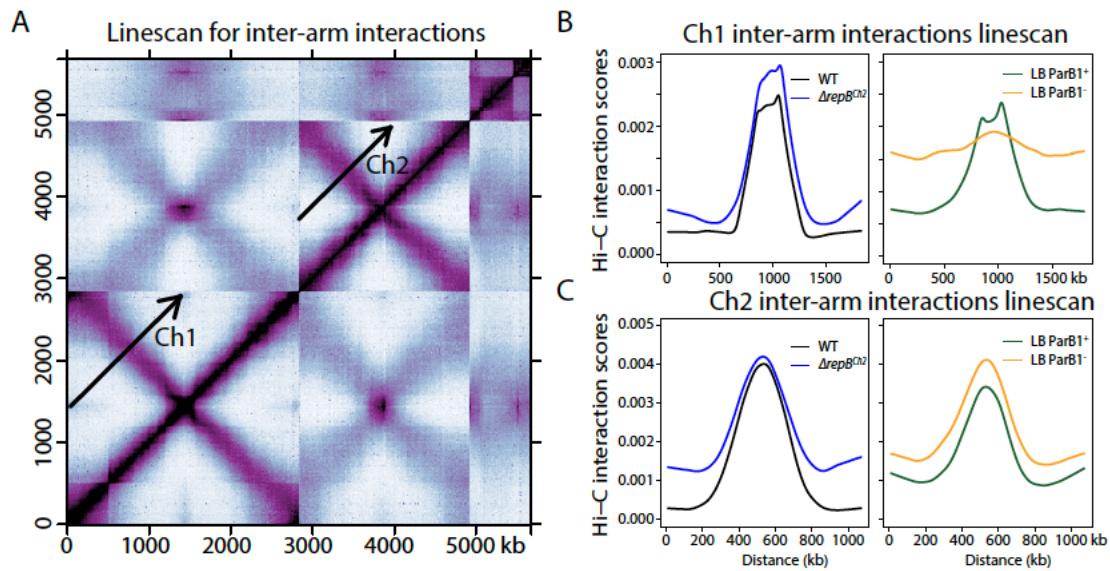


Fig. S5. Quantification of inter-arm interactions. (A) To quantify the inter-arm interactions on Ch1, a line was drawn from the coordinate (0 kb, 1850 kb) on the left y-axis to the coordinate (1000 kb, 2850 kb) on the top boundary of Ch1, parallel to the primary diagonal, crossing the secondary diagonal emanated from *ori1*. Similarly, to quantify the Ch2 interactions, a line was drawn from the coordinate (2850 kb, 3920 kb) to the coordinate (3850 kb, 4920 kb). The arrowheads indicate the direction of the plot on the x-axis in (B-C). The Hi-C interaction scores along these lines were plotted for the indicated strains. (B) Ch1 inter-arm interactions in WT (Fig. 1B) and $\Delta repB^{Ch2}$ (ATWX089, Fig. 3C) grown in ATGN (left panel) and in ParB1⁺ and ParB1⁻ (AtWX192 with or without AHL and theophylline) grown in LB (Fig. 3AB) (right panel). (C) Ch2 inter-arm interactions of the same strains grown in the same conditions.

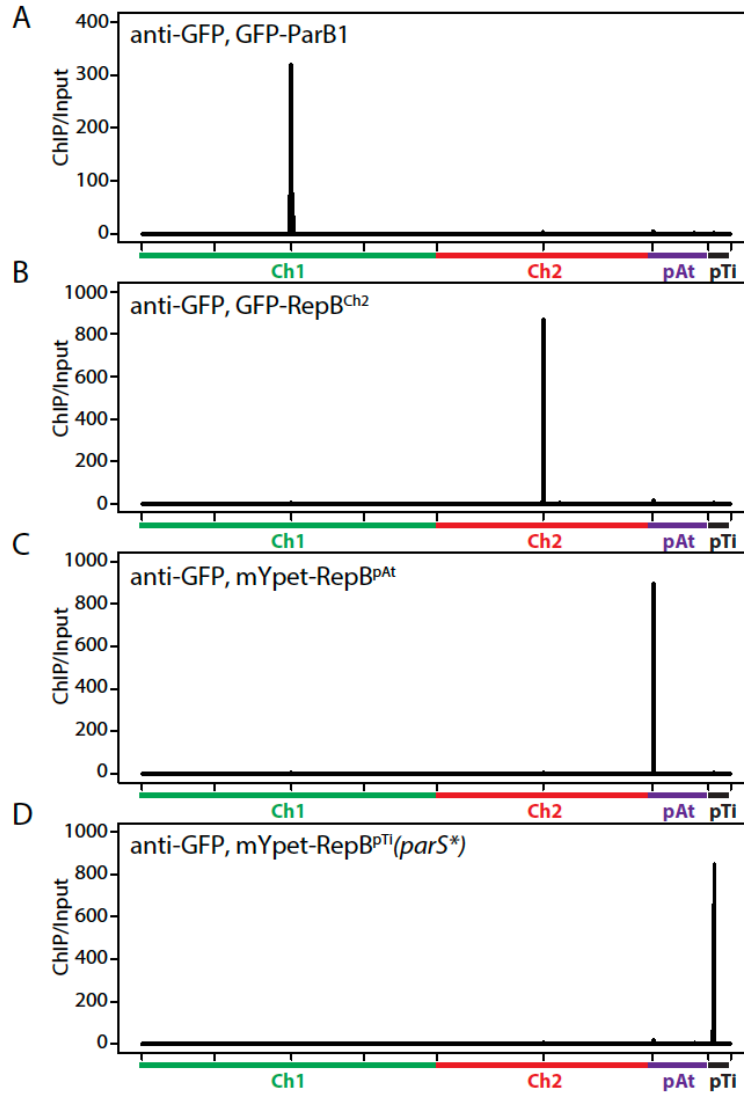


Fig. S6. The binding sites of GFP/mYpet fusions to ParB1 or RepBs. ChIP enrichment of (A) GFP-ParB1 (AtWX226), (B) GFP-RepB^{Ch2} (AtWX228), (C) mYpet-RepB^{pAt} (AtWX179), (D) mYpet-RepB^{pTi} (*parS**) (AtWX372) expressed from pSRKKm-based plasmids. Fluorescent fusions were induced using 0.25 mM IPTG for 4 hours before harvesting for ChIP. x-axis shows genome positions and y-axis indicates ChIP enrichment in 1-kb bins. ParB1 and RepB fusions are only enriched at the origins of their cognate replicons.

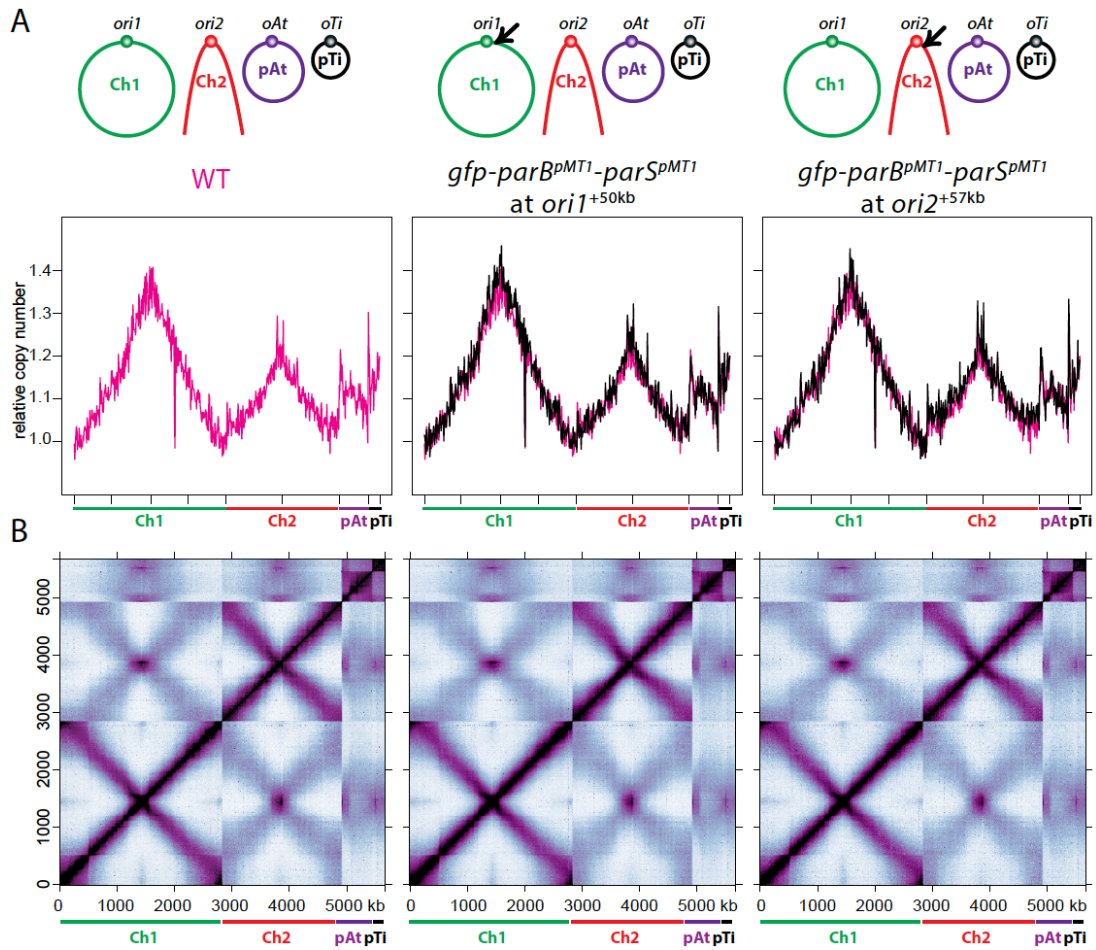


Fig. S7. The presence of *gfp-parB^{pMT1}-parS^{pMT1}* cassette did not alter DNA replication or genome organization. (A) Top panels illustrate the genomes of the three strains used: WT (AtWX063 left), *gfp-parB^{pMT1}-parS^{pMT1}* visualization cassette inserted at 50 kb clockwise from *ori1* (AtWX278 middle) or at 57 kb clockwise from *ori2* (AtWX295 right). Black arrows indicate the insertion points of the cassette. Bottom panels show the genome-wide copy number using WGS. Result from WT is plotted in magenta. On the middle and right panels, results of the indicated strains are plotted in black, on top of the WT plot in magenta. The WGS profiles of indicated strains are very similar to that of the WT, indicating that the presence of the visualization cassette did not alter DNA replication. (B) Normalized Hi-C maps of the same three strains. The presence of the *gfp-parB^{pMT1}-parS^{pMT1}* visualization cassette did not alter genome organization.

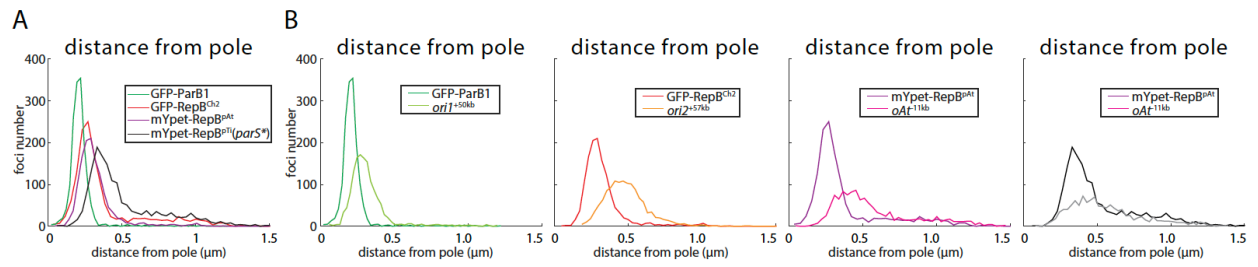


Fig. S8. Hierarchy of origin localization. (A) Distance of ParB1- and RepB-labeled origins from the nearest cell pole. (B) Comparison of ParB1/RepB-labeled origins with pMT1 system-labeled origins.

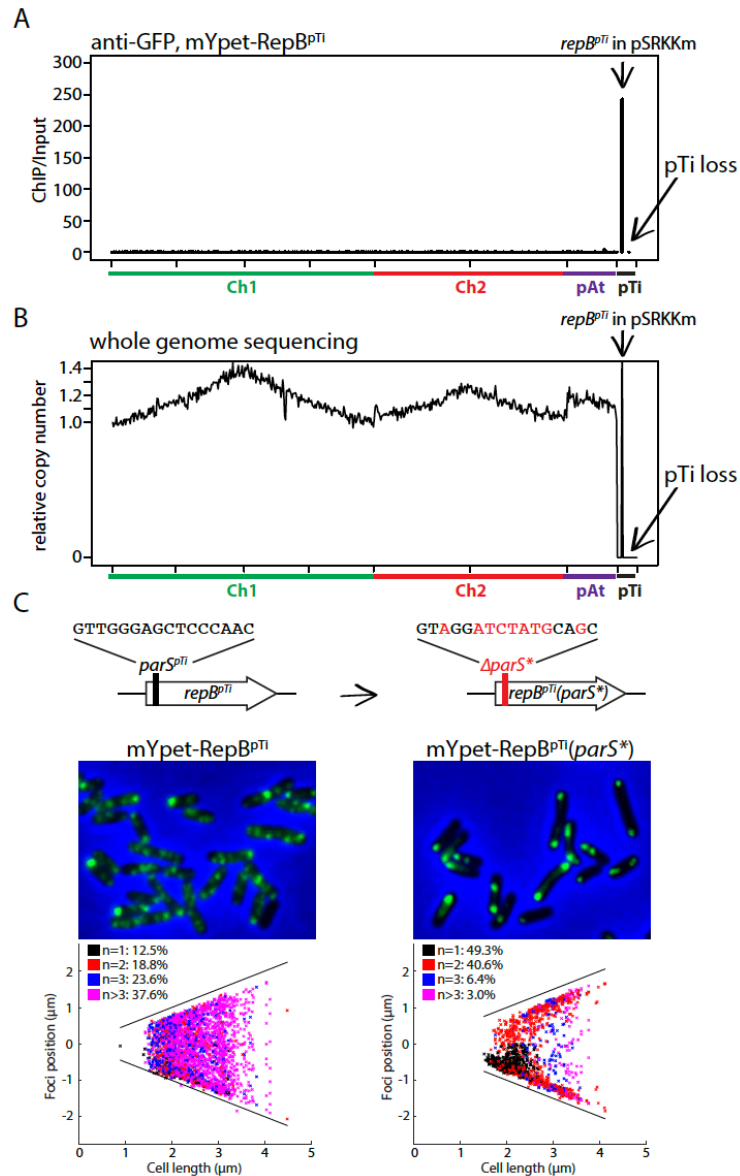


Fig. S9. pTi was lost in the strain expressing mYpet-RepB^{pTi}. (A-B) ChIP enrichment of mYpet-RepB^{pTi} (ChIP/input) or whole genome sequencing of AtWX181 (pSRKKm *plac mypet-repB^{pTi}*) plotted in 1-kb bins. x-axis shows genome positions and y-axis indicates ChIP enrichment (A) or relative copy number (B). The only bins with values above backgrounds were at the gene locus of *repB^{pTi}* that was also present in the pSRKKm plasmid. Other bins on pTi had no values, indicating pTi was lost in the cells. (C) Top, a *parS* site of RepB^{pTi} was present inside the *repB^{pTi}* gene. Point mutations (19) were introduced to mutate the *parS^{pTi}* site without changing the amino acid sequence of RepB^{pTi}. Middle, microscopy images of mYpet-RepB^{pTi} (AtWX181) and mYpet-RepB^{pTi}(parS*) (AtWX372). Bottom, plots showing relative position of the foci. 1000 cells were analyzed for each strain. The solid black lines indicate the positions of two poles. The percentage of cells containing 1 (black), 2 (red), 3 (blue) or greater than 3 (magenta) foci are shown. In Figures A-C, the fluorescent fusions was induced using 0.25 mM IPTG for 4 hours.

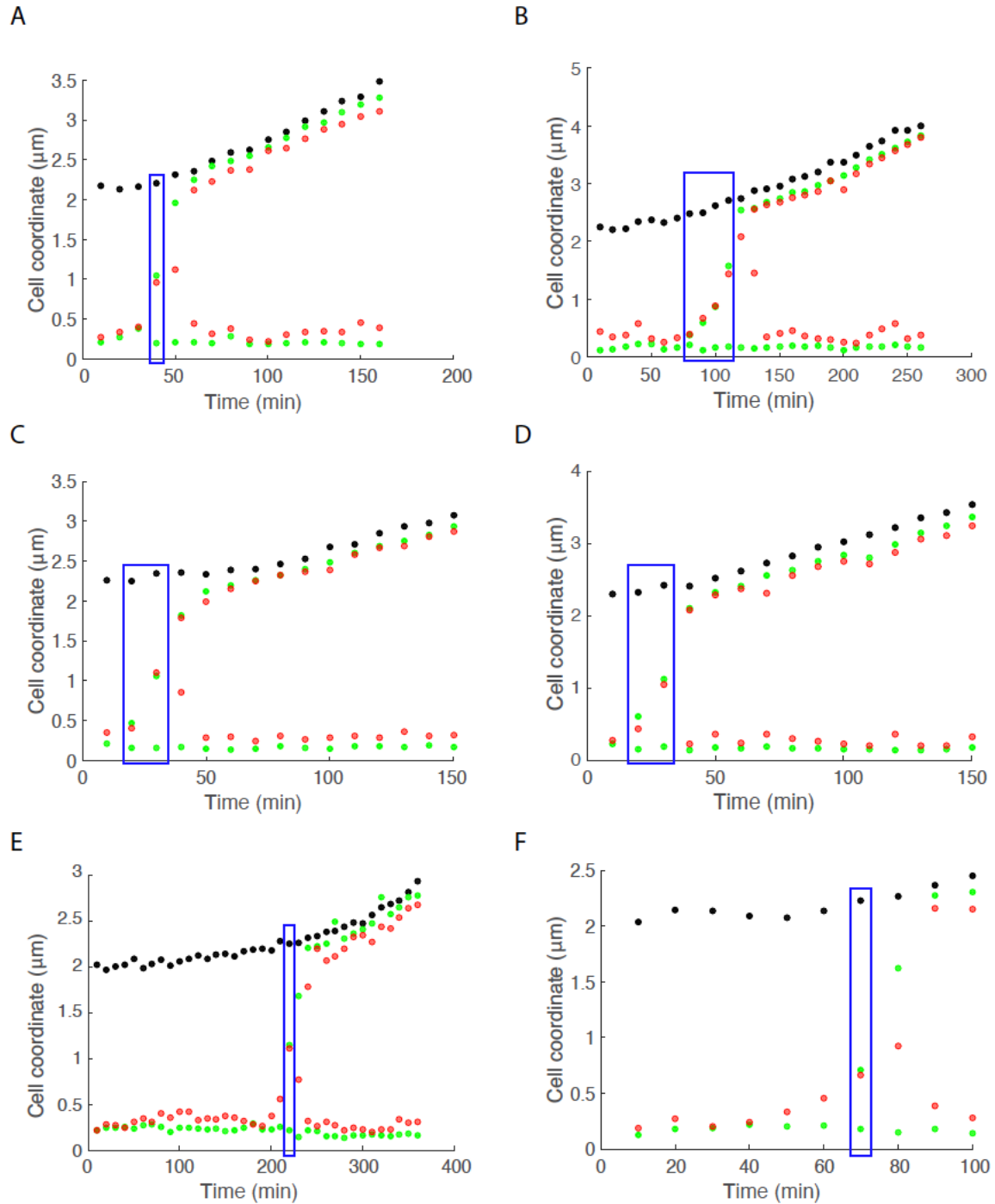


Fig. S10. During segregation, single *ori2* focus (likely unreplicated) is frequently co-localized with the moving *ori1* focus. (A-F) Six examples of Type 1 cells presented in Figure 4A. On the y-axis, 0 μm positions indicate the old cell poles. Black, green and red dots indicate the new cell poles, *ori1* foci and *ori2* foci, respectively. Blue boxes indicate the frames in which a single *ori2* focus is colocalized with the moving *ori1* focus. (A) is the plotting the data presented in Fig. 4A. In our microscopy images, the fluorescent foci have an average radius of 6 pixels ($0.39 \mu\text{m}$). On plots shown in this figure, the dots indicate the center of the fluorescent foci; the dots that are less than $0.39 \mu\text{m}$ apart appear as overlapping foci in the images.

Table S1. Bacterial strains used in this study.

Strain	Genotype	Reference	Figure
A. tumefaciens used in main figures			
AtWX063	C58, wild type		1B, 2A, 2B, 2FG, 3E, S1A-D, S2E, S3B, S4A-D, S5A-C, S7AB
AtWX108	C58, Δsmc (Atu0801/ATU_RS03945)	This study	1E, 2F, S3AB
AtWX192	C58, <i>tetRA::gen Ptral-riboswitch-parB1</i> (Atu2828/ATU_RS13770) <i>traR</i> , clone 1	This study	2CD, 2FG, S4EF, S4IJ, S4MN, S5BC
AtWX089	C58, $\Delta repB^{Ch2}$ (Atu3923/ATU_RS18280)::amp	This study	2E-G, S5BC
AtWX226	C58, pSRKKm <i>msfgfp-parB1</i> (Atu2828/ATU_RS13770) (<i>kan</i>)	This study	3A, S6A, S8AB
AtWX228	C58, pSRKKm <i>msfgfp-repB^{Ch2}</i> (Atu3923/ATU_RS18280) (<i>kan</i>)	This study	3A, S6B, S8AB
AtWX179	C58, pSRKKm <i>mypet-repB^{pAt}</i> (Atu5001/ATU_RS23955) (<i>kan</i>)	This study	3A, S6C, S8AB
AtWX372	C58, pSRKKm <i>mypet-repB^{pTi}</i> (<i>parS*</i>) (Atu6044/ATU_RS23220) (<i>kan</i>)	This study	3A, S6D, S8AB, S9C
AtWX181	C58, pSRKKm <i>mypet-repB^{pTi}</i> (Atu6044/ATU_RS23220) (<i>kan</i>)	This study	S9A-C
AtWX278	C58, <i>ygfp-parB^{MT1}-parS^{MT1}</i> inserted between Atu0047/ATU_RS00230 and Atu0048/ATU_RS00235 50 kb from <i>ori1</i>	This study	3B-D, S7AB, S8B
AtWX295	C58, <i>ygfp-parB^{MT1}-parS^{MT1}</i> inserted between Atu3973/ATU_RS18530 and Atu3974/ATU_RS18535 57 kb from <i>ori2</i>	This study	3B-D, S7AB, S8B
AtWX359	C58, <i>ygfp-parB^{MT1}-parS^{MT1}</i> inserted between Atu5336/ATU_RS25500 and Atu5337/ATU_RS25505 11 kb from <i>oAt</i>	This study	3B-D, S8B
AtWX351	C58, <i>ygfpP-parB^{MT1}-parS^{MT1}</i> inserted between Atu6047/ATU_RS23235 and Atu6048/ATU_RS23240 4 kb from <i>oTi</i>	This study	3B-D, S8B
AtWX263	C58, pSRKKm <i>Plac rfp-repB^{Ch2}</i> (Atu3923/ATU_RS18280) terminator <i>Plac egfp-parB1</i> (Atu2828/ATU_RS13770) terminators	This study	4A-C, S10A-F
AtWX319	C58, pSRKKm <i>Plac rfp-repB^{pAt}</i> (Atu5001/ATU_RS23955) terminator <i>Plac egfp-parB1</i> (Atu2828/ATU_RS13770) terminators	This study	4D
Strains used for strain building or in supplemental figures			
AtWX050	15955, wild-type	(21)	S2ABF
AtWX113	C58, $\Delta tral$ (Atu6042: ATU_RS23210)	This study	
AtWX167	C58, $\Delta tral$ (Atu6042: ATU_RS23210), <i>tetRA::gen Ptral-riboswitch-parB1</i> (Atu2828/ATU_RS13770) <i>traR</i>	This study	
AtWX193	C58, <i>tetRA::gen Ptral-riboswitch-parB1</i> (Atu2828/ATU_RS13770) <i>traR</i> , clone 2	This study	S4GH, S4KL
IB124	15955, pAt15955 Δ 270, pTi15955-cured	(20)	S2CG
IBE13A	15955, pAt15955 Δ 270, pTi15955	(20)	S2D

IBJUN138	15955, pTi15955-cured	(20)	S2H
----------	-----------------------	------	-----

Table S2. Plasmids used in this study.

Plasmid	Description	Reference
pWX820	pSRKKm <i>msfgfp-parB1</i> (Atu2828/ATU_RS13770) (<i>kan</i>)	This study
pWX821	pSRKKm <i>msfgfp-repB^{Ch2}</i> (Atu3923/ATU_RS18280) (<i>kan</i>)	This study
pWX832	pNPTS138 Δ <i>smc</i> (Atu0801/ATU_RS03945) (<i>kan</i>)	This study
pWX844	pSRKKm <i>mYpet-repB^{Ch2}</i> (Atu3923/ATU_RS18280) (<i>kan</i>)	This study
pWX854	pNPTS138 Δ <i>repB^{Ch2}</i> (Atu3923/ATU_RS18280):: <i>amp</i> (<i>kan</i>)	This study
pWX879	pMiniTn7 <i>Ptral MCS traR</i> (Atu6134: ATU_RS23655) (<i>gen</i>)	This study
pWX885	pMiniTn7 <i>Ptral-riboswitch-parB1</i> (Atu2828/ATU_RS13770) <i>traR</i> (Atu6134: ATU_RS23655) (<i>gen</i>)	This study
pWX902	pNPTS138 <i>tetRA::gen Ptral-riboswitch-parB1</i> (Atu2828/ATU_RS13770) <i>traR</i> (<i>kan</i>)	This study
pWX905	pSRKKm <i>mypet-repB^{pAt}</i> (Atu5001/ATU_RS23955) (<i>kan</i>)	This study
pWX906	pSRKKm <i>mypet-repB^{pTi}</i> (Atu6044/ATU_RS23220) (<i>kan</i>)	This study
pWX914	pNPTS138 Δ <i>parB1</i> (Atu2828/ATU_RS13770):: <i>amp</i> (<i>kan</i>)	This study
pWX915	pACYC terminators Ppen	
pWX917	pACYC terminators Ppen <i>ygfp-parB^{MT1}-parS^{MT1}</i>	This study
pWX924	pACYC terminators Ppen <i>ygfp-parB^{MT1}-parS^{MT1} terminators</i>	This study
pWX931	pNPTS138 Ppen <i>ygfp-parB^{MT1}-parS^{MT1}</i> at Atu3054/ATU_RS14060	This study
pWX950	pNPTS138 PT7strong <i>ygfp-parB^{MT1}-parS^{MT1}</i> at Atu3054/ATU_RS14060	This study
pWX963	pNPTS138 PT7strong <i>ygfp-parB^{MT1}-parS^{MT1}</i> at Atu0048/ATU_RS00235	This study
pWX967	pNPTS138 PT7strong <i>ygfp-parB^{MT1}-parS^{MT1}</i> at Atu3973/ATU_RS18530	This study
pWX970	pSRKKm <i>Plac rfp-repB^{Ch2}</i> (Atu3923/ATU_RS18280) <i>terminator Plac egfp-parB1</i> (Atu2828/ATU_RS13770) <i>terminators</i>	This study
pWX974	pSRKKm <i>Plac rfp-repB^{pAt}</i> (Atu5001/ATU_RS23955) <i>terminator Plac egfp-parB1</i> (Atu2828/ATU_RS13770) <i>terminators</i>	This study
pWX1004	pNPTS138 <i>ygfp-parB^{MT1}-parS^{MT1}</i> at Atu6047/ATU_RS23235	This study
pWX1005	pNPTS138 <i>ygfp-parB^{MT1}-parS^{MT1}</i> Atu5337/ATU_RS25505	This study
pWX1025	pSRKKm <i>mypet-repB^{pTi}</i> (<i>parS*</i>) (Atu6044/ATU_RS23220) (<i>kan</i>)	This study
pACE001	pSRKKm <i>Plac rfp-repB^{Ch2}</i> (Atu3923/ATU_RS18280)	(17)
pFHC2973	pALA2705 derivative; <i>Plac cfp-parB^{P1} ygfp-parB^{MT1}</i>	(14)
pHP45omega	<i>omega-amp</i> cassette	(11)

pJW101	pNPTS138 $\Delta tral$ (Atu6042: ATU_RS23210) (<i>kan</i>)	This study
pJZ254	pSRKKm <i>Plac egfp-parB1</i> (Atu2828/ATU_RS13770)	(17)
pJZ274	pBluescript II SK <i>sacB</i> native <i>RBS</i> of <i>gpr::riboswitch</i>	(13)
pNPTS138	<i>oriT sacB kan</i>	(9)
pSRKKm	Broad host-range, <i>Plac</i>	(7)
pSRKKm <i>msfgfp</i>	pSRKKm <i>Plac msfgfp</i>	(8)
pTD114	pBBR1MCS-5 derivative; <i>Plac::traR Ptral</i>	(12)
pUC18-mini-Tn7T-GM-Plac-HA	pUC18-mini-Tn7T gen <i>Plac HA</i>	(8)
pWX361	<i>ycgO::PftsW tetR-cfp (spec) terminators PftsW lacI-mypet</i>	(10)

Table S3. Oligonucleotides used in this study.

Oligo	Sequence	Use
oWX486	gccgctctagctaagcagaaggc	sequencing
oWX1835	gccagggtttcccagtcacga	sequencing
oWX1854	cgccagggtttcccagtcacgac	sequencing
oWX1855	tcacacaggaaacagctatgac	sequencing
oWX2017	tggcgccaagcttctctgcaggatagccggaagccagaggctattcc	pWX914, sequencing
oWX2020	gctagcgaattcgtggatccagatcatgccgcttaccaccgatcag	pWX914, sequencing
oWX2021	tggcgccaagcttctctgcaggatcaggcgcagaacttctacgatgc	sequencing
oWX2024	gctagcgaattcgtggatccagatcgcgagagacaattgctgtttg	sequencing
oWX2031	gaactgggtgtagcgtcgttaagc	sequencing
oWX2044	caattcacacaggaaacagcatatgagtaaagggaagaactgttcacc	pWX820, pWX821
oWX2046	ggatcctccagatccttgtatagttcatccatgccgtg	pWX820, pWX821
oWX2047	tatacaaaggatctggaggatccagtgatgatcttctgaagcgtcgattg	pWX820
oWX2048	ctcgaggtcgacggatcgcgataagctttatttctgctccagcagccggcagac	pWX820
oWX2049	tatacaaaggatctggaggatccagcagaaaacagatattcgccaatc	pWX821
oWX2050	ctcgaggtcgacggatcgcgataagcttctcactgcttgaccggattcggcaaac	pWX821
oWX2060	ggaaagcgggcagtgagcgc	sequencing
oWX2061	gaaggttatgtacaggagcgcacc	sequencing
oWX2076	tggcgccaagcttctctgcaggatagcacagagtgccgatttaag	pWX854
oWX2077	gctagcgaattcgtggatccagatctaaccgccatgccacctcc	pWX854
oWX2081	tggcgccaagcttctctgcaggatggaactgcctgaatccaccg	pWX832
oWX2082	gtctgcaaattccacggagacgagcttgtgaacttcatgc	pWX832
oWX2083	gcatgaagttcaacaagctcgtctccgtggattgcagac	pWX832
oWX2084	gctagcgaattcgtggatccagatggtgaatagctggagcagcc	pWX832
oWX2085	cgacttcatcatcaacggc	sequencing
oWX2086	tgacgagcacaggaatgagg	sequencing
oWX2169	caattcacacaggaaacagcatatgtctaaagggaagaattattc	pWX844, sequencing
oWX2171	ggcgaatatctgtttctgctggatcctccagatccttgtacaattcattcatacc	pWX844
oWX2173	tagacacaacattgaagatggtgg	sequencing

oWX2206	aaataaacaataggggtccgcaagattggcgaatatctgtt	pWX854
oWX2207	gcctcactgattaagcattggtaaacgctgtttgccgaataccg	pWX854
oWX2210	cgcggaaccctattgttta	pWX854
oWX2211	ttaccaatgcttaatcagtgaggc	pWX854
oWX2265	accgaacaggcttatgtcaagtcgactaatacgcactactataggg	pWX879, sequencing
oWX2266	ataggtactcaagtcattagctagccgaattaatgtgagttagc	pWX897
oWX2268	ctttgagtgaggtggccaaggatccttattctgctccagcagcc	pWX885
oWX2273	gttcaagttcgaactgcg	sequencing
oWX2276	caatgttcatgcgagaagcgatcgc	sequencing
oWX2277	ccgatagtgaaactcgggccg	sequencing
oWX2279	ctgattccagttcaacgctctgacc	sequencing
oWX2280	gcacgacacagaagagagtgatcc	sequencing
oWX2288	cgctacgtttctgggctagcccgggatacgcactactatagacc	pWX885
oWX2289	ttcgaagatcatcactcatctgttgataccccctgccc	pWX885
oWX2290	gcgcaggggatcaacaagatgagtgatgatctttcgaa	pWX885
oWX2337	atacgactcactatagaccgggtataccagcatcgtctt	sequencing
oWX2342	gcagcttctctcataccggctagcgcactcctgttgatagatccag	pWX902, sequencing
oWX2343	caaggcgagaagataaagtgccatggcgaattaatgtgagttagc	pWX902, sequencing
oWX2348	caagttcccagaggaatcgg	sequencing
oWX2349	ggtgatcgatctcgatcggg	sequencing
oWX2351	gaattgggtaccgggccccccctcgagttaagtctttgatccctgcccc	pWX905
oWX2353	gaattgggtaccgggccccccctcgagctattggtcgagcttgcctcctcc	pWX906
oWX2377	ggcttctttgttatcaagcgcag	sequencing
oWX2378	gtgccagacgaaatggttcag	sequencing
oWX2379	cttttccatcagctctgttaccg	sequencing
oWX2380	aaataaacaataggggtccgcaatcgacgcttcgaaagatcatc	pWX914
oWX2381	gatgatctttcgaagcgtcgattgcgcaaccctattgtttattt	pWX914
oWX2382	ctccagcagccggcagacggcttctaccaatgcttaatcagtgaggc	pWX914
oWX2383	gcctcactgattaagcattgtaagaagcgtctgccggctgctggag	pWX914
oWX2391	aatcaaatattcaagctaaaggaggtgaaacatgtctaaaggtgaagaactgtttac	pWX917
oWX2392	caaaaaagatgctcttcggcatcctctcgagtactcacctgattctggaagtc	pWX917
oWX2393	gactccagaatcaggtgagtaactcgagaggatgccgaagacatctttttg	pWX917
oWX2394	cgatactgcagatgocagatggatcccgcgaattatgagtcacgaagag	pWX917

oWX2395	tcttcgctattacgccagatcc	sequencing
oWX2396	ccgtcaattgtctgattcgttacc	sequencing
oWX2397	gatgacggtaactacaaaaccc	sequencing
oWX2403	catggatccatgtcgacagactctctagcttgaggcatc	pWX924
oWX2404	gctcagccggccgtcaacgttcttgccattgctgca	pWX924
oWX2405	gaactttacaagggatctggaggatccaccagtaagtcacgcgtaaatcc	pWX905
oWX2406	ctttacaagggatctggaggatccgccaggggtgcagttgtcttcttg	pWX906
oWX2407	ctctagatagcgcgatgctgaattc	pWX931, pWX963, pWX967, pWX1004, pWX1005, sequencing
oWX2408	ggttatgctagtattgctcagcc	pWX931, pWX963, pWX967, pWX1004, pWX1005, sequencing
oWX2420	ggcgccaagcttctctgcaggatatccagttacgtgctggcggcaggatc	pWX931
oWX2421	gaattcagcatgcgctatctagagctattttgggatagctcgaaccgtg	pWX931
oWX2422	ggctgagcaataactagcataaccggcaggcatatgaaaccggattg	pWX931
oWX2423	ctagcgaattcgtggatccagatatctgcatgtggaacgatggtgaggg	pWX931
oWX2424	ttctgccgctccgatcaaaacagg	sequencing
oWX2425	ccggactccacatccgcagatttc	sequencing
oWX2426	ggccttctgcttagctagagcggc	sequencing
oWX2431	taatacgactcactatagggagaccacaacgcttcatctggttacgatcaatc	pWX950
oWX2432	ggctcccctatagtgagtcgtattaatttcgaaatgatgacctcgtttccacc	pWX950
oWX2502	cgccaagcttctctgcaggatatcgaacgtcgatattggcctcgaatg	pWX963
oWX2503	aattcagcatgcgctatctagagtcagcccgcctgctttgctttcag	pWX963
oWX2504	ggctgagcaataactagcataaccagcggccgctggtatttcag	pWX963
oWX2505	tagcgaattcgtggatccagatatctcgggttatgcgctgccggcc	pWX963
oWX2506	acaatattggcctgatggaggacc	sequencing
oWX2507	aaaagggacaggacacgctgtcc	sequencing
oWX2508	cgccaagcttctctgcaggatatcaacgcgcgaaaaactgttgacg	pWX967
oWX2509	aattcagcatgcgctatctagagtcagcgtccgtgctgtttgcgcc	pWX967

oWX2510	gctgagcaataactagcataacctcgttctcaaagttggtcgattg	pWX967
oWX2511	agcgaattcgtggatccagatatcgacactggaggatagggaaacattc	pWX967
oWX2512	cccaccaacctcaccaaacacgag	sequencing
oWX2513	tccgtgcaggagatcgcttccttc	sequencing
oWX2520	tcaagctagagagtctgctagcaattcgaaagcaaattcg	pWX970
oWX2521	ccccgccgaagcgggggttttttaagcttctactgcttgaccgg	pWX970
oWX2522	cggtcgaaattgcttgcgaattgctagcagactcttagcttgaggcatc	pWX970, sequencing
oWX2523	attaatgaatcggccaacgcttcaacgttctgccattgctgc	pWX970
oWX2524	gcaatggcaagaacgttgaagcgttgccgattcattaatgc	pWX970, sequencing
oWX2525	agcttaaaaaaacccccgcttcggcgggggtttttttatttctgctccagcagccgg	pWX970
oWX2535	taaaagcttaaaaaaacccccgcttcgg	pWX974
oWX2536	catcctagggcgccggtggag	pWX974
oWX2539	caacgaggactacaccatcgtgg	sequencing
oWX2540	cgccgaagcgggggttttttaagctttaaagcttctgatcccttcgcg	pWX974
oWX2541	ggccgccactccaccggcgcccctaggatgaccagtaagtcatcgcg	pWX974
oWX2593	gcgccaagcttctctgcaggatatcaacgaagaggacaactgtttcgc	pWX1004
oWX2594	ggaattcagcatgcgctatctagagtcaaatacaacccccatgcacgg	pWX1004
oWX2595	cggtgagcaataactagcataacctgtgaaggcagaaacatggtcgg	pWX1004
oWX2596	tagcgaattcgtggatccagatatctataacgaagcggctcggc	pWX1004
oWX2597	cgccaagcttctctgcaggatatccagggatggcattaaggtcc	pWX1005
oWX2598	cgcggggaattcagcatgcgctatctagagtcaagtctccttgaggtcgctg	pWX1005
oWX2599	acggccggctgagcaataactagcataacccccaaaaaacgttctcctccagcc	pWX1005
oWX2600	agcgaattcgtggatccagatatccttcgccaacgtgctggatgcc	pWX1005
oWX2712	tctgtaggatctagtcagccaagcgcatttgcaatcaaaaatgcg	pWX1025
oWX2713	cttgctgactagatcctacaagacaagacaactgcaccctggc	sequencing

Table S4. Next generation sequencing samples used in this study.

Sample name	Figure	Reference	Identifier
401_Wang_HiC_AtWX063_ATGN	1B, S1A-D, S3A, S4A, S5A	this study	GSM5542437
402_Wang_HiC_AtWX108_ATGN	1E, S3A	this study	GSM5542438
403_Wang_input_AtWX063_ATGN_rep2	2AB	this study	GSM5542439
404_Wang_ChIP_anti_AtParB_AtWX063_ATGN	2A	this study	GSM5542440
405_Wang_ChIP_anti_AtRepBCh2_AtWX063_ATGN	2B	this study	GSM5542441
406_Wang_HiC_AtWX192_LB_AHL_Theo	2C, S4I, S5BC	this study	GSM5542442
407_Wang_HiC_AtWX192_LB	2D, S4J, S5BC	this study	GSM5542443
408_Wang_HiC_AtWX089_ATGN	2E, S5BC	this study	GSM5542444
409_Wang_WGS_AtWX063_ATGN_rep1	3E	this study	GSM5542445
410_Wang_HiC_AtWX050_ATGN	S2A	this study	GSM5542446
411_Wang_HiC_AtWX050_virulence	S2B	this study	GSM5542447
412_Wang_HiC_IB124_virulence	S2C	this study	GSM5542448
413_Wang_HiC_IBE13A_virulence	S2D	this study	GSM5542449
414_Wang_HiC_AtWX063_LB_rep2	S2E	this study	GSM5542450
415_Wang_HiC_AtWX050_LB	S2F	this study	GSM5542451
416_Wang_HiC_IB124_LB	S2G	this study	GSM5542452
417_Wang_HiC_IBJun138_LB	S2H	this study	GSM5542453
418_Wang_HiC_AtWX063_ATGN_AHL	S4B	this study	GSM5542454
419_Wang_HiC_AtWX063_ATGN_Theo	S4C	this study	GSM5542455
420_Wang_HiC_AtWX063_ATGN_AHL_Theo	S4D	this study	GSM5542456
421_Wang_HiC_AtWX192_ATGN_AHL_Theo	S4E	this study	GSM5542457
422_Wang_HiC_AtWX192_ATGN	S4F	this study	GSM5542458
423_Wang_HiC_AtWX193_ATGN_AHL_Theo	S4G	this study	GSM5542459
424_Wang_HiC_AtWX193_ATGN	S4H	this study	GSM5542460
425_Wang_HiC_AtWX193_LB_AHL_Theo_rep2	S4K	this study	GSM5542461
426_Wang_HiC_AtWX193_LB	S4L	this study	GSM5542462
427_Wang_ChIP_antiGFP_AtWX181_ATGN_250uMIPTG4h	S9A	this study	GSM5542463
428_Wang_input_AtWX181_ATGN_250uMIPTG4h	S9AB	this study	GSM5542464
429_Wang_HiC_AtWX192_LB_12h	S4N	this study	GSM5689546
430_Wang_ChIP_anti_GFP_AtWX226_ATGN_250uMIPTG4h	S6A	this study	GSM5689547
431_Wang_input_AtWX226_ATGN_250uMIPTG4h	S6A	this study	GSM5689548
432_Wang_ChIP_anti_GFP_AtWX228_ATGN_250uMIPTG4h	S6B	this study	GSM5689549
433_Wang_input_AtWX228_ATGN_250uMIPTG4h	S6B	this study	GSM5689550
434_Wang_ChIP_anti_GFP_AtWX179_ATGN_250uMIPTG4h	S6C	this study	GSM5689551
435_Wang_input_AtWX179_ATGN_250uMIPTG4h	S6C	this study	GSM5689552
436_Wang_ChIP_anti_GFP_AtWX372_ATGN_250uMIPTG4h	S6D	this study	GSM5689553
437_Wang_input_AtWX372_ATGN_250uMIPTG4h	S6D	this study	GSM5689554
438_Wang_WGS_AtWX063_ATGN_rep2	S7A	this study	GSM5689555
439_Wang_WGS_AtWX278_ATGN	S7A	this study	GSM5689556
440_Wang_WGS_AtWX295_ATGN	S7A	this study	GSM5689557
441_Wang_HiC_AtWX278_ATGN	S7B	this study	GSM5689558
442_Wang_HiC_AtWX295_ATGN	S7B	this study	GSM5689559

SI References

1. X. Wang *et al.*, Condensin promotes the juxtaposition of DNA flanking its loading site in *Bacillus subtilis*. *Genes Dev* **29**, 1661-1675 (2015).
2. D. Z. Rudner, P. Fawcett, R. Losick, A family of membrane-embedded metalloproteases involved in regulated proteolysis of membrane-associated transcription factors. *Proc Natl Acad Sci U S A* **96**, 14765-14770 (1999).
3. J. Livny, Y. Yamaichi, M. K. Waldor, Distribution of centromere-like *parS* sites in bacteria: insights from comparative genomics. *J Bacteriol* **189**, 8693-8703 (2007).
4. U. M. Pinto, K. M. Pappas, S. C. Winans, The ABCs of plasmid replication and segregation. *Nat Rev Microbiol* **10**, 755-765 (2012).
5. A. Paintdakhi *et al.*, Oufiti: an integrated software package for high-accuracy, high-throughput quantitative microscopy analysis. *Mol Microbiol* **99**, 767-777 (2016).
6. N. Feirer *et al.*, A Pterin-Dependent Signaling Pathway Regulates a Dual-Function Diguanylate Cyclase-Phosphodiesterase Controlling Surface Attachment in *Agrobacterium tumefaciens*. *mBio* **6**, e00156 (2015).
7. S. R. Khan, J. Gaines, R. M. Roop, 2nd, S. K. Farrand, Broad-host-range expression vectors with tightly regulated promoters and their use to examine the influence of TraR and TraM expression on Ti plasmid quorum sensing. *Appl Environ Microbiol* **74**, 5053-5062 (2008).
8. W. Figueroa-Cuilan, J. J. Daniel, M. Howell, A. Sulaiman, P. J. Brown, Mini-Tn7 Insertion in an Artificial attTn7 Site Enables Depletion of the Essential Master Regulator CtrA in the Phytopathogen *Agrobacterium tumefaciens*. *Appl Environ Microbiol* **82**, 5015-5025 (2016).
9. A. J. Hinz, D. E. Larson, C. S. Smith, Y. V. Brun, The *Caulobacter crescentus* polar organelle development protein PodJ is differentially localized and is required for polar targeting of the PleC development regulator. *Mol Microbiol* **47**, 929-941 (2003).
10. X. Wang, P. Montero Llopis, D. Z. Rudner, *Bacillus subtilis* chromosome organization oscillates between two distinct patterns. *Proc Natl Acad Sci U S A* **111**, 12877-12882 (2014).
11. R. Fellay, J. Frey, H. Krisch, Interposon mutagenesis of soil and water bacteria: a family of DNA fragments designed for in vitro insertional mutagenesis of gram-negative bacteria. *Gene* **52**, 147-154 (1987).
12. T. Danhorn, M. Hentzer, M. Givskov, M. R. Parsek, C. Fuqua, Phosphorus limitation enhances biofilm formation of the plant pathogen *Agrobacterium tumefaciens* through the PhoR-PhoB regulatory system. *J Bacteriol* **186**, 4492-4501 (2004).
13. J. R. Zupan, R. Grangeon, J. S. Robalino-Espinosa, N. Garnica, P. Zambryski, GROWTH POLE RING protein forms a 200-nm-diameter ring structure essential for polar growth and rod shape in *Agrobacterium tumefaciens*. *Proc Natl Acad Sci U S A* **116**, 10962-10967 (2019).
14. H. J. Nielsen, J. R. Ottesen, B. Youngren, S. J. Austin, F. G. Hansen, The *Escherichia coli* chromosome is organized with the left and right chromosome arms in separate cell halves. *Mol Microbiol* **62**, 331-338 (2006).
15. A. B. Dalia, T. N. Dalia, Spatiotemporal Analysis of DNA Integration during Natural Transformation Reveals a Mode of Nongenetic Inheritance in Bacteria. *Cell* **179**, 1499-1511 e1410 (2019).
16. W. M. Figueroa-Cuilan *et al.*, Diversification of LytM Protein Functions in Polar Elongation and Cell Division of *Agrobacterium tumefaciens*. *Frontiers in Microbiology* **12** (2021).

17. J. S. Robalino-Espinosa, J. R. Zupan, A. Chavez-Arroyo, P. Zambryski, Segregation of four *Agrobacterium tumefaciens* replicons during polar growth: PopZ and PodJ control segregation of essential replicons. *Proc Natl Acad Sci U S A* **117**, 26366-26373 (2020).
18. E. R. Morton, C. Fuqua, Laboratory maintenance of *Agrobacterium*. *Curr Protoc Microbiol* **Chapter 1**, Unit3D 1 (2012).
19. R. P. Simon, U; Pühler, Alfred, A Broad Host Range Mobilization System for In Vivo Genetic Engineering: Transposon Mutagenesis in Gram Negative Bacteria. *Nature Biotechnology* **1**, pages 784–791 (1983).
20. I. S. Barton, T. G. Platt, D. B. Rusch, C. Fuqua, Destabilization of the Tumor-Inducing Plasmid from an Octopine-Type *Agrobacterium tumefaciens* Lineage Drives a Large Deletion in the Co-resident At Megaplasmid. *G3 (Bethesda)* **9**, 3489-3500 (2019).
21. Y. Dessaux, J. Tempe, S. K. Farrand, Genetic analysis of mannityl opine catabolism in octopine-type *Agrobacterium tumefaciens* strain 15955. *Mol Gen Genet* **208**, 301-308 (1987).